OPEN ACCESS

DEVELOPMENT OF THE METHOD FOR CALCULATING THE LIFTING CAPACITY OF UNITS MOUNTED ON A SELF-PROPELLED TRACTOR-TYPE CHASSIS

Volodymyr Krasnokutskyi[1][0000-0001-9484-4113], Mikhail Podryhalo[2][0000-0002-1624-5219], Serhii Selevych[1][0009-0005-2162-4992], Vadym Kaviuk[3][0000-0002-0367-8314], Oleksandr Krasnokutskyi[4][0009-0001-9484-0742], Boris Kalchenko[1][0000-0003-3827-1693]
[1]National Technical University "Kharkiv Polytechnic Institute", Kharkiv, Ukraine
[2]Kharkiv National Automobile and Highway University, Kharkiv, Ukraine
[3]Ivan Kozhedub Kharkiv National Air Force University, Kharkiv, Ukraine
[4]National Defense University of Ukraine, Kyiv, Ukraine
Email: serhii.selevych@khpi.edu.ua

Abstract - An analysis was carried out on studies evaluating the load-carrying capacity of machines and implements depending on gravity forces and external resistances, types of loads, and their redistribution during the performance of various types of work. The problem of determining the maximum permissible weight of the aggregated machine was solved, taking into account the specific features of the unit's formation. Graphs of the potential load-carrying capacity, its characteristics, and the dependencies of the maximum weight values are presented.
The loads acting on the unit in both static and dynamic states were investigated. An evaluation of the unit's load-carrying capacity was performed based on an analysis of its dynamic component. A graphical analysis of the obtained results was carried out. It was shown that, under the influence of rolling resistance moments, the coordinate of the maximum load shifts toward the axis of the front wheels, resulting in their partial unloading.

Keywords: Tractor self-propelled chassis, Traction dynamics, load characteristics, Inter-axle mounting, Mounted machine, Rolling resistance.

1. Introduction

An analysis of the research on the traction dynamics of tractor self-propelled chassis (TSPCH) when aggregated with mounted machines using inter-axle mounting and methods for calculating the traction of tractors and TSPCH are presented in [1] and serve as benchmarks for evaluating their traction characteristics. These calculations are mainly employed to assess their performance with trailed or mounted machines [2]. When TSPCH is coupled with mounted equipment via inter-axle mounting, it encounters a system of forces and moments in the longitudinal-vertical plane that influences its coupling and traction-power parameters. Consequently, standard traction calculation indicators for TSPCH are inadequate for analyzing mounted machines configured with inter-axle mounting. Traction calculations generally presume a constant TSPCH weight [3]. However, when mounted equipment is added to the inter-axle zone, the equipment's weight increases the overall load, while the vertical soil reaction on the operational bodies becomes a contributing factor. Additionally, variations in the mounted machine's design and coupling method significantly affect the force impact on TSPCH and the extent of additional weight. The positioning of the mounted machine on the TSPCH frame further alters the coupling weight of the unit. While tractors face restrictions in mass redistribution to maintain stability and maneuverability, TSPCH benefits from additional loading on both axles due to the machine's weight within the basic inter-axle mounting space [3]. Adjustments in the total and coupling weight of TSPCH within the aggregate directly influence track formation, which in turn alters rolling resistance.

2. Literature Review

Studies published in [5-7] indicate that less than 60–70% of a tractor engine's power is converted into

https://doi.org/10.17683/ijomam/issue22.v1.16

traction force for agricultural implements, with this efficiency dropping to as low as 50% on soft, loose soils. Research in [8] reveals that approximately 20–55% of the available axle power of a tractor is consumed by tire-soil interactions, primarily due to rolling resistance and drive wheel slippage. Studies in [9, 10] emphasize the adoption of modern technologies, such as traction control systems, ballast weights, and low-pressure tires, to minimize slippage. Additionally, tire slippage is strongly correlated with the tractor's coefficient of adhesion, which is defined as the drawbar pull divided by the total force acting on the drive tires in a direction perpendicular to the contact surface.

In [11], the efficiency of an all-wheel-drive mini electric tractor was analyzed, focusing on the optimal distribution of weight across the tractor axles and internal tire pressure to enhance performance. To address the growing need for efficient power transmission from the engine to the drawbar while minimizing environmental impact, a modern traction wheel, the "wheel with rigid support," was introduced in [12]. This innovation significantly enhanced traction without increasing equipment weight. By enabling the use of wider implements, it also reduced field movement intensity and soil compaction.

The slippage efficiency of a tractor with mechanical front-wheel drive during soil tillage was examined in [13]. The findings revealed a 21% non-linear reduction in slippage efficiency, with the slippage coefficient of the rear wheels increasing relative to the front wheels. Additionally, the total traction force of the rear wheels rose compared to the front wheels. In [14], a methodological analysis of energy dissipation by the wheels of a front-wheel-drive tractor during plowing operations showed that energy dissipation accounted for approximately 25% of the total energy expenditure for plowing. A method for predicting the slippage of tractor drive tires, incorporating numerical expressions for tire pressure, was developed in [15]. An empirical equation derived from this study allowed for theoretical predictions of drive tire slippage in both 4WD and 2WD modes.

Research in [16] outlined methods to improve traction efficiency by optimizing the distribution of vertical reactions between the wheels, particularly in tractors with unstable coupling mass. Key principles for assessing the traction properties of such tractors were also formulated. Additionally, [17] investigated the loads on agricultural aggregates during unsteady motion while performing technological operations, highlighting an 8% discrepancy between the maximum theoretical traction force and the force measured using the proposed experimental methodology.

Based on these studies, it has been established that the redistribution of normal reactions between the axles of TSPCH in an aggregate significantly influences the rolling conditions of the front and rear axle wheels, resulting in varying rolling resistance forces. Traditional traction calculation methods are inadequate for fully capturing the range of potential traction loads for TSPCH in a mounted aggregate, as they are limited by the adhesion constraints of the drive wheels to the soil.

3. Development Methodology

3.1. Load-Carrying capacity of Assemblies based on a TSPCH

According to the nature of the reactions acting on the wheels of TSPCH and on the working elements, which arise from the effects of gravity and external resistances, mounted machines are divided into two main groups: those that generate reactions on the wheels only due to the action of gravity, and those that generate reactions on the wheels due to both gravity and external environmental resistance.

Machines and implements of the second group can, in transport position, formally be classified as belonging to the first group. For the overwhelming majority of units, all types of loads may be considered symmetrical relative to the central longitudinal (conditional) plane of symmetry of the TSPCH.

It may be assumed that all units (except transport units) operate at speeds below 15 km/h, which limits the dynamic loads on the wheels and allows the use of the tire load-carrying capacity reserve provided by the applicable standard. In practice, the degree of utilization of tire load capacity is typically assessed by static reactions, since it is difficult to account for the dynamic redistribution of loads for each specific operating condition.

Redistribution of loads to the rear axle of the TSPCH under working conditions increases the corresponding reactions by approximately 10%. According to experimental data from the Research Institute of Large-Size Tires, tire overloading within these limits reduces tire service life by about 20%. Therefore, when forming a unit, it is necessary to consider the loads arising under both static and dynamic conditions, and to use in calculations the loads corresponding to the case of maximum loading.

To enable evaluation of the load-carrying capacity of the units, their static state is considered for machines of both groups using a common methodology, which is then refined based on analysis of the corresponding dynamic state.

When analyzing load-carrying capacity, it is first necessary to determine the dependence of the limiting weight values of the machines on the position of the unit’s center of gravity, based on the maximum permissible load values on the TSPCH wheel tires in static conditions. Taking into account

the load-carrying capacities of the front and rear wheel tires and the corresponding load-carrying capacity adjustment coefficients, the permissible additional loading of the axles when attaching machines and implements is as follows for the front axle:

$$Q_f - G_f = 2q_f k_f - G_f, \quad (1)$$

where Q_f – permissible additional load on the front axle when attaching machines and implements; G_f – weight acting on the front wheels; q_f – load-carrying capacity of a front wheel; k_f – load-carrying capacity coefficient for the front wheels;

for the rear axle:

$$Q_r - G_r = 2q_r k_r - G_r, \quad (2)$$

where Q_r – permissible additional load on the rear axle when attaching machines and implements; G_r - weight acting on the rear wheels; q_r – load-carrying capacity of a rear wheel; k_r – load-carrying capacity coefficient for the rear wheels;

Considering the TSPCH as a simply supported beam resting on the wheel axles, we can examine the corresponding loading schemes. The reactions resulting from the action of the weight of the aggregated machine G_R on the front wheels are as follows:

$$R_f = G_R \frac{L - a_m}{L} \leq 2q_f k_f - G_f, \quad (3)$$

where R – rated tractive effort; L – wheelbase (longitudinal distance between axles); a_m – longitudinal coordinate of the center of gravity of the mounted implement;

for the rear axle:

$$R_r = G_R \frac{a_m}{L} \leq 2q_r k_r - G_r \quad (4)$$

The maximum permissible weight of the aggregated machine $G_{v,\max}$ and the corresponding coordinate $a_{v,\max}$ at full tire loading are equal to

$$G_{v,max} = 2\left(q_f k_f + q_r k_r\right) - G_C, \quad (5)$$

where $G_{v,\max}$ – weight of the mounted machine or implement; G_C – operational weight of the TSPCH;

$$a_{m,max} = L \frac{2q_r k_r - G_r}{2(q_f k_f + q_r k_r) - G_C} \quad (6)$$

where $a_{m,\max}$ – longitudinal coordinate of the center of gravity of the mounted machine or implement;

For any other position of the mounted machine, its weight and the longitudinal coordinate of its center of gravity can be calculated using the following formulas:

Case 1: When the load-carrying capacity of the unit is limited only by the load-carrying capacity of the steering (front) wheels:

$$R_f = 2q_f k_f - G_f \quad (7)$$

where R_f – is the reaction on the front wheels due to the weight of the aggregated machine;

$$R_r \leq 2q_r k_r - G_r \quad (8)$$

from which:

$$G_R = \frac{L}{L - a_m}(2q_r k_r - G_r); \quad (9)$$

where a_m – is the longitudinal coordinate of the center of gravity of the mounted machine or implement;

$$a_m \leq L \frac{2q_r k_r - G_r}{2(q_f k_f + q_r k_r) - G_C} \quad (10)$$

Case 2: When the load-carrying capacity of the unit is limited only by the load-carrying capacity of the drive (rear) wheels:

$$R_f \leq 2q_f K_f - G_f \quad (11)$$

where K_f – is the adjustment coefficient for the load-carrying capacity of the front wheels;

$$R_r = 2q_r K_r - G_r \quad (12)$$

where K_r – is the adjustment coefficient for the load-carrying capacity of the rear wheels;

from which:

$$G_m = \frac{L}{a_m}(2q_r K_r - G_r); \quad (13)$$

$$a_m \geq L \frac{2q_r K_r - G_r}{2(q_f K_f + q_r K_r) - G_C}; \quad (14)$$

The obtained dependencies can be analysed on graphs, for the TSPCH T-16MG under the most typical inter-axle mounting. For the T-16MG chassis, the front wheel tires are 170-406 (6.0/16) according to the tire standard (DSTU 4140:2020), with $q_f = 550$ MPa at a pressure of 0.32 MPa. For operation on soft soils, $q_f = 395 \div 430$ Pa at a pressure of 0.18–0.21 MPa. The rear wheels use tires 240-830 (9.5/9–32) with $q_r = 780 \div 865$ MPa at a pressure of 0.13–0.15 MPa; for operation on soft

soils, $q_r = 595 \div 720$ MPa at a pressure of 0.08–0.11 MPa.

The standard allows for an increase in the load-carrying capacity of tires at operating speeds below 16 km/h by 35% for steering (front) wheels and 20% for drive (rear) wheels at the same tire pressure. Accordingly, the tire load-carrying capacity adjustment coefficients are $k_f = 1.35$ and $k_r = 1.2$. The load limitation ($k_f = k_r = 1$) applies to transport units based on the TSPCH.

The input values for the calculations are: $L = 2500$ mm; $G_f = 260$ kgf; $G_r = 1400$ kgf; $G_C = 1600$ kgf (weight of the chassis with a rigid protective frame).

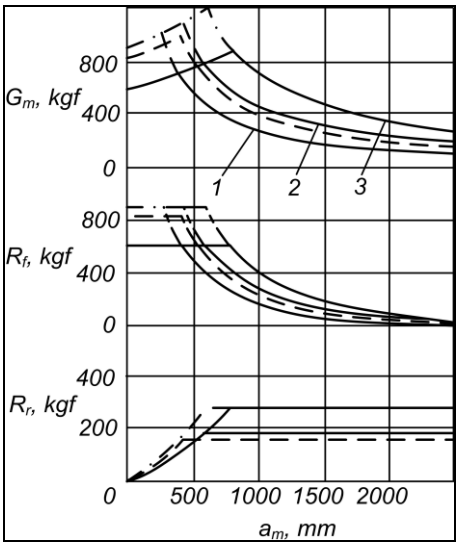

Figure 1: Characteristic of the potential load-carrying capacity of the TSPCH T-16MG: solid lines – load-carrying capacity of the chassis on soft soil at drive-wheel tire pressures of 0.09, 0.11, and 0.10 MPa (curves 1, 2, and 3, respectively) and steering-wheel tire pressure of 0.21 MPa; dash-dot lines – same conditions, but with the use of the reserve load-carrying capacity of the steering-wheel tires; dashed lines – load-carrying capacity of the chassis during transport operations (drive-wheel tire pressure 0.13 MPa; steering-wheel tire pressure 0.32 MPa).

The nominal load-carrying capacity of the TSPCH drive wheels at a pressure of 0.08–0.1 MPa (field conditions) does not ensure proper operation of the units ($q_r < 0.5G_r$). Therefore, when performing unitization calculations, the reserve load capacity of the tires must be considered.

3.2. Steady-state Operation for a TSPCH with Mounted Machine

When constructing the load-carrying capacity characteristics of the TSPCH for transport operations, the nominal tire load-carrying capacity at a pressure of 0.15 MPa is used.

Figure 1 shows the dependencies of the limiting weight of the aggregated machine on the horizontal coordinate of its center of gravity $G_R = f_1(a_R)$; the additional load on the front wheels $R_f = f_2(a_R)$and on the rear wheels $R_r = f_3(a_R)$ at the limiting values of G_R, where, f_1 is the reduced rolling resistance coefficient for the entire unit, f_2 is the reduced rolling resistance coefficient for the front wheels, f_3 is the reduced rolling resistance coefficient for the rear wheels.

The curves describe the variation of the total reactions on the respective axles can be determined from the following relationships (for the interaxial mounting):

in the range $[0 \div a_{R,\max}]$:

$$Y_{f\,st} = [2q_f k_f \div G_r + \frac{a_m}{L-a_m}(2q_f k_f - G_f)] \quad (15)$$

Where $Y_{f,st}$is the normal soil reaction on the front wheels under static conditions; $Y_{r,st}$ is the normal soil reaction on the rear wheels under static conditions;

in the range $[a_{m,\max} \div L]$:

$$Y_{r\,st} = [2q_r k_r \div G_f + \frac{L-a_m}{a_m}(2q_r k_r - G_r)] \quad (16)$$

When the machines and implements are mounted within the range $[0 \div a_{R,\max}]$, the value of $G_R$is limited by the load-carrying capacity of the front wheels, while the rear wheels cannot be fully loaded by the machine's weight. When the center of gravity of the mounted machine is located within the range $[a_{R,\max} \div 2500\,\text{mm}]$, full loading of the rear wheels can be achieved while the front wheels remain underloaded. For a given value of the machine weight relative to the front wheels in the working position G'_m, the equations of load-carrying capacity of the steering and driving wheels yield the range of possible positions of the machine on the TSPCH frame.

$$a_{m1} = L(1 - \frac{2q_f k_f - G_f}{G_R}) \le a_R \le a_{m2} = L\frac{2q_r K_r - G_r}{G_r} \quad (17)$$

When the reserve load-carrying capacity of the tires is used ($k_f > 1$ and $k_r > 1$), this range increases.

The obtained data can be refined based on the analysis of the steady operation of the TSPCH with machines of the first group on a horizontal surface. In this case, the tractive resistance of the unit

represents a component of the rolling resistance force.

The normal dynamic reactions on the front (Y_{fd}) and rear (Y_{rd}) axles can be determined from the following equations:

$$Y_{fd} = \frac{G_v(L-a_v)-M_{rf}-M_{rr}}{L} = \frac{G_r(L-a_v)-M_R+X_f(r_r-r_f)}{L}, \quad (18)$$

where G_v – operating weight of the unit; a_v– longitudinal coordinate of the unit's center of gravity; M_{rf} – rolling resistance moment of the front wheels; M_{rr} – rolling resistance moment of the rear wheels; M_R– rolling resistance moment of the entire unit; X_f – rolling resistance of the front wheels; r_r – dynamic radius of the rear wheel; r_f – dynamic radius of the front wheel.

$$Y_{rd} = \frac{G_v a_v-M_{rf}-M_{rr}}{L} = \frac{G_v a_v+M_R+X_f(r_r-r_f)}{L} \quad (19)$$

To determine the value of the total rolling resistance moment of the unit $(M_{rf}+M_{rr})$, both sides of the traction balance equation of the unit are multiplied by the dynamic radius of the driving wheel.

$$P_T r_r = [P_E + (Y_{fd}+Y_{rd})f]r_r, \quad (20)$$

where P_T – tangential traction force; P_E – tractive effort corresponding to the nominal engine power;

or

$$M_r = P_E r_r + M_{rf}\frac{r_r}{r_f} + M_{rr}, \quad (21)$$

where M_r is the total rolling resistance moment of the unit. After transformation, we obtain:

$$P_{rr} r_r = M_{rf} + M_{rr} + \frac{M_{rf}}{r_f}(r_r - r_f), \quad (22)$$

where P_{rr} – is the rolling resistance force, However, since

$$P_{rr} = (Y_{rr}+Y_{rd})f_1 = G_v f_1 \text{ and } \frac{M_{rf}}{r_f} = Y_{fd} f_2 \quad (23)$$

from this

$$M_{rf} + M_{rr} = G_v f_1 r_r - Y_{fd} f_2 (r_r - r_f) \quad (24)$$

3.3. Limiting Weight of the Aggregated Machine

When calculating with the relatively small term $R_f(r_r - r_f)$, the value of the reduced rolling resistance coefficient can be used with sufficient accuracy. Under this assumption, substituting $M_{rf}+M_{rr}$into formulas (18) and (19) yields:

$$Y_{fd} = \frac{G_v(L-a_p-fr_r)}{L-f(r_к-r_f)}; Y_{rd} = \frac{G_v(a_p+fr_r)}{L-f(r_к-r_f)}. \quad (25)$$

To ensure normal operating conditions, the following constraints must be satisfied:

$$Y_{fd} \le 2q_f k_f; \; Y_{rd} \le 2q_r k_r. \quad (26)$$

Since $Y_{fd}+Y_{rd} = G_v$, it follows that $G_{md,\max} = G_{m,\max}$, i.e., the maximum permissible weight of the aggregated machine in this case does not change.

Considering that

$$a_v = \frac{\sum(G_i a_i)}{\sum G_i} = \frac{G_c a_c + G_{md}\, a_{md}}{G_c + G_{md}}$$
$$\text{and,} \quad (27)$$
$$G_v = \sum G_i = G_c + G_{md}$$

where G_{md} – is the maximum weight of the aggregated machine;

For inter-axle mounting, the longitudinal coordinate of the center of gravity of the mounted machine at maximum weight in the working state, $a_{md,\max}$, taking into account $Y_{rd} = \frac{(G_v(a_v+fr))}{(L-f_1(r_r-r_f))} = 2\,q_r k_r$ and the known values of a_p and G_v, can be written as:

$$a_c + G_{md}a_{md} + f_1 r_f (G_C + G_{fd}) = \\ = 2q_r k_r [L - f(r_r - r_f)]. \quad (28)$$

Substituting the value of the maximum weight of the mounted machine $G_{md,max} = 2q_f k_f + 2q_f k_f - G_c$, and solving for $a_{md,max}$, gives:

$$a_{md,max} = \frac{L\left(2q_r k_r - \frac{G_c a_c}{L}\right) - 2f_1(q_f k_f r_f + q_r k_r r_r)}{2\,q_f k_f + 2p_r k_r - G_c} \quad (29)$$

since

$$\frac{G_c a_c}{L} = G_r \text{ and } \frac{L(2q_r k_r - G_r)}{G_{m,max}} = a_{m,max} \quad (30)$$

we have:

$$a_{md,max} = \frac{2q_r k_r L - G_c a_c - f_1(2q_f k_f r_f + 2q_r k_r r_r)}{2(q_f k_f + q_r k_r) - G_c} = \\ = L\frac{2q_r k_r - G_r}{G_{m,max}} - \frac{2\,G_1(q_f k_f r_f + q_r k_r r_r)}{2(q_f k_f + q_r k_r) - G_c} = \\ a_{m,max} - \frac{2f_1(q_f k_f r_f + q_r k_r r_r)}{2(q_f k_f + q_r k_r) - G_c} \quad (31)$$

It is noteworthy that the value of $a_{md,\max}$ is less than $a_{m,\max}$. Under the action of rolling resistance

moments, the coordinate of the peak of the maximum load shifts toward the axis of the steering wheels. This is logical, as it results in partial unloading of the front wheels.

The maximum permissible weight of the aggregated machine, G_{md}, when the center of gravity of the mounted machine is located to the left of $a_{md,max}$, is determined from:

$$Y_{fd} = \frac{G_v(L - a_v - f_1 r_r)}{L - f(r_r - r_f)} = 2 q_f k_f \quad (32)$$

Solving this equation for G_{md}, after substituting the values of G_v and a_m, we obtain:

$$G_{md} = \frac{L\left[2q_f k_f - \left(G_c - \frac{G_c a_c}{L}\right)\right] + G_c f_1 r_r - 2q_f k_f f_1 (r_к - r_п)}{L - a_m - f_1 r_к} = \\ = \frac{L(2q_r k_r - G_r) + G_c f_1 r_r - 2q_f k_f f (r_r - r_f)}{L - a_m f r_r} \quad (33)$$

When the center of gravity of the mounted machine is located to the right of $a_{md,max}$, from the equation

$$Y_{зд} = \frac{G_v(a_v + f_1 r_f)}{L - f_1(r_к - r_f)} = 2 q_r k_r \quad (34)$$

then

$$G_{md} = \frac{L(2q_r k_r - G_r) + G_c f_1 r_f - 2q_r k_r f_1 (r_r - r_f)}{a_m + f_1 r_r}, \quad (35)$$

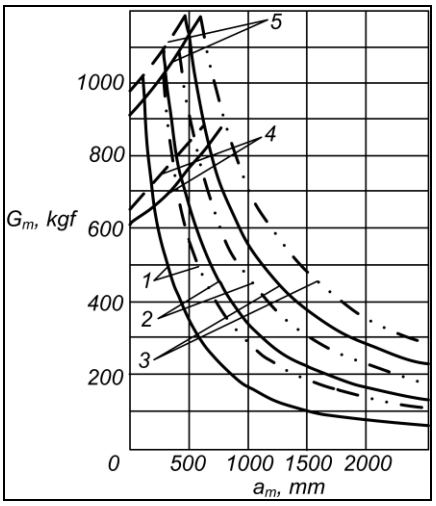

Figure. 2: Dependence of the maximum weight of the attached machine on the horizontal coordinate of its center of gravity (for static and dynamic conditions): solid lines – the general envelope for the considered case; dash-dot lines – curves plotted under the condition of static force action; 1, 2, and 3 – for the load-carrying capacity of the driving wheel tires on soft soil at pressures of 0.09, 0.10, and 0.11 MPa, respectively; 4 and 5 – for the nominal and maximum load-carrying capacity of the steering wheel tires at a pressure of 0.21 MPa; G_f=260 kgf; G_r = 1400 kgf; f_1 = 0,12

Based on the obtained data, it is possible to adjust the potential limits of the mounting zone on the chassis. When determining the loads on the front wheels of the unit, it is sufficient to consider only the static forces, whereas for the rear wheels, the dynamic redistribution of loads must be taken into account. As a result, the range of possible positions of the center of gravity of a machine with a given weight G'_m is narrowed and lies within the following limits:

$$a_{m1} = L\left(1 - \frac{2q_f k_f - G_f}{G'_m}\right) \le a_m \le a_{m2} = \\ = \frac{L(2q_r k_r - G_r) + G_c f_1 r_f - 2q_r k_r f_1 (r_r - r_f)}{G'_н} - f_1 r_f \quad (36)$$

Figure 2 shows the dependencies of the maximum weight of the aggregated machine on the horizontal coordinate of its center of gravity. As described above, the allowable load-carrying capacity region of the TSPCH on the graph is obtained by superimposing the curves of static and dynamic loading.

The curves are plotted for conditions of operation on compacted plowed soil, which practically covers the full range of tasks performed by TSPCHs of this class with first-group machines in crop production (dusting, spraying, vegetable harvesting with harvesting platforms, etc.). Under these conditions, the dynamic redistribution of loads significantly limits the effective load-carrying capacity of the drive axle of the chassis.

At the same time, for a transport unit based on the TSPCH (Fig. 3), the operational load-carrying capacity is close to the static value. This is due to the relative reduction of rolling resistance moments as a result of the wheels rolling over compacted soil. In this case, the maximum weight of the transport unit can be estimated based on the static load-carrying capacity of the TSPCH.

3.4. Features of Unit Formation based on a TSPCH

Features of unit formation with second-group machines in the working position. In this case, it is necessary to determine the magnitude and direction of the total reaction on the working elements. Its magnitude, direction, and point of application depend on the type of agricultural work being performed, the structural design, the condition of the working elements, soil conditions, and a number of other factors.

For most soil-working machines, the point of application of the total reaction lies approximately in the longitudinal-vertical symmetry plane passing through the center of gravity of the unit.

For design calculations, it is convenient to use the horizontal (R_X) and vertical (R_Y) components of the total reaction. The horizontal component is determined based on the structural parameters of the machine's working elements and the specific resistances characteristic of machines of that type. The calculation method for determining the horizontal component is fairly universal, as experimental characteristics of the specific resistances of all aggregatable machines have been developed and reported in the literature for optimal speed levels, fully covering the range of soil processing depth adjustments. To determine R_u, experimental data on the ratio of horizontal and vertical reaction components are used, for example, data from dynamometer measurements of soil reactive resistance on the working elements.

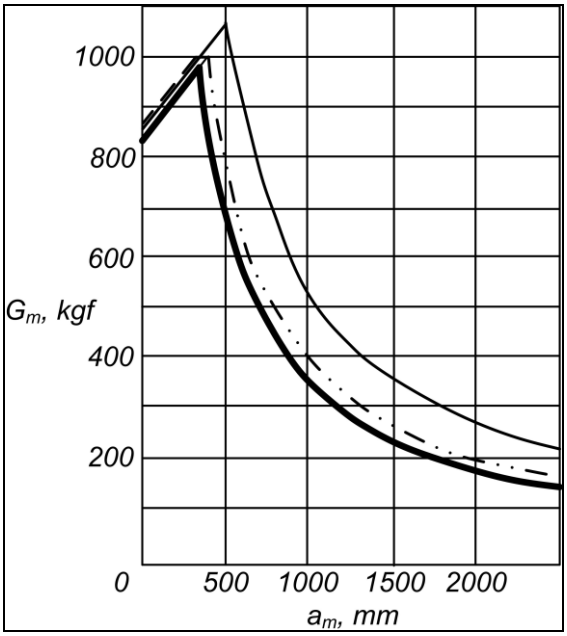

Figure 3: Load-Carrying Capacity Characteristics of the T-16MG Transport Chassis (for Static and Dynamic Conditions): solid bold line – the general envelope for the considered case; dash-dot lines – the curve plotted under the condition of static force action; dashed lines – the same, but under motion; solid line – the curve of the static load-carrying capacity of the T-16MG chassis (without the rigid protective frame); – components of the reactions, for example, data from dynamometer measurements of the soil reactive resistance acting on the working elements.

For the positional and power-based mounting methods, a rigid power connection exists between the machine and its working elements with the chassis frame. Taking into account the forces acting on the unit in the longitudinal plane during steady operation on a horizontal surface, the normal reactions on the TSSH wheels can be expressed by the following equations:

$$Y'_{fd} = \frac{G_v(L-a_v)-(M_{rf}+M_{rr})}{L} \pm R_y\left(1-\frac{a_r}{L}\right) \quad (37)$$

where Y'_{fd} – is the nominal reaction on the front wheels of the TSSH, considering the forces acting on the unit in the longitudinal plane during steady operation on a horizontal section; R_y – is the vertical component of the resultant reaction acting on the working elements;

$$Y'_{rd} = \frac{G_v a_v+M_{rf}+M_{rr}}{L} \pm R_y\frac{a_r}{L} \quad (38)$$

where a_r – is the distance from the line of action of R_y to the vertical plane passing through the axis of the front wheels; Y'_{rd} - is the nominal reaction on the rear wheels of the TSSH, considering the forces acting on the unit in the longitudinal plane during steady operation on a horizontal section.

By comparing the obtained expressions for Y'_{fd} and Y'_{rd} with those previously presented for Y_{fd} and Y_{rd}, it can be seen that the selection of G_v and the coordinate a_v primarily depends on the sign of R_y.

When $R_y \le 0$, the calculation should be carried out for the transport position of the machine, and when $R_y > 0$, the values of G_m and a_m have additional constraints. In this case:

$$M_{rf}+M_{rr} = M_r - P_E r_r - X_f(r_r - r_f) = \\ = (G_v + R_y)fr_r - Y'_{fd}f_1(r_r - r_f) \quad (39)$$

since $Y'_{fd}+Y'_{rd} = G_v + R_y$ and $X_f = Y'_{fd}f_1$. As before, when calculating for the relatively small quantity $X_f(r_r - r_f)$, the value of the reduced rolling resistance coefficient is used. Taking this into account:

$$Y'_{fd} = \frac{G_v(L-a_v-f_1r_r)+R_y(L-a_r-f_1r_r)}{L-f_1(r_r-r_f)} = \\ = Y_{fd} + R_y\frac{(L-a_r-f_1r_r)}{L-f_1(r_r-r_f)} \quad (40)$$

$$Y'_{rd} = \frac{G_v(a_r+f_1r_r)+R_y(a_r+f_1r_r)}{L-f_1(r_r-r_f)} = \\ = Y_{rd} + R_y\frac{(a_r+f_1r_r)}{L-f_1(r_r-r_f)} \quad (41)$$

Since $Y'_{fd} \le 2q_f k_f$ and $Y'_{rd} \le 2q_r k_r$, and taking into account that the coordinate a_r can always be represented as the algebraic sum of a_v and a specific value e for each given machine (where e is the horizontal distance from the center of gravity of the machine to the point of application of the reaction on the working elements), after transformations we can obtain the following results for the interaxle (mid-mounted) hitch:

1. Maximum value of the permissible (limit) weight of the aggregated machine and the coordinate of the center of gravity of the mounted machine at this limit weight in working condition:

$$G'_{md\,max} = 2\left(q_f k_f + q_r k_r\right) - G_c - R_y = \\ = G_{vd\,max} - R_y \quad (42)$$

where $G'_{md\,max}$ is the maximum permissible weight of the operationally aggregated machine.

$$a'_{md\,max} = \frac{L(2q_r k_r - G_r) - f_1\left(2q_f k_f r_f + 2q_r k_r r_r\right)}{2\left(q_f k_f + q_r k_r\right) - G_c} - \\ - \frac{R_y e}{2\left(q_f k_f + q_r k_r\right) - G_c =} = a_{md\,max} - \frac{R_y e}{G_{md\,max}} \quad (43)$$

where $a'_{md\,max}$ is the coordinate of the center of gravity of the mounted machine. These parameters are determined from the system of equations:

$$\frac{G_v(a_v + f_1 r_f) + R_y(a_r + f_1 r_f)}{L - f_1(r_r - r_f)} = 2q_r k_r \quad (44)$$

$$G'_{md\,max} = 2\left(q_f k_f + q_r k_r\right) - G_c - R_y \quad (45)$$

by substituting the values

$$a_p = \frac{G_c a_c + G'_{vd\,max} a'_{vd\,max}}{G_c + G'_{vd\,max}},\ G_v = G_c + G'_{md\,max} \quad (46)$$

If it is assumed that the line of action of R_y passes through the center of gravity of the mounted machine, then $a'_{md\,max} = a_{md\,max}$. This is due to the proportional distribution of the vertical reaction across the supports, which leads to a corresponding decrease in the specific weight of the aggregated machine.

2. From the equation:

$$\frac{G_v(L - a_v - f_1 r_r) + R_y(L - a_r - f_1 r_r)}{L - f_1(r_r - r_f)} = 2q_r k_r \quad (47)$$

the limit weight of the aggregated machine is determined when its center of gravity is to the left of the point $a'_{vd\,max}(a_v < a'_{vd\,max})$:

$$G'_{md} = \frac{L\left(2q_f k_f - G_f\right) + G_c f_1 r_r - 2q_f k_f f_1\left(r_r - r_f\right)}{L - a_m - f r_r} - \\ - R_y\left(1 + \frac{e}{L - a_m - f r_r}\right) = \\ = G_{md} - R_y\left(1 + \frac{e}{L - a_m - f r_r}\right) \quad (48)$$

3. Similarly, from the equation $Y'_{fd} = 2q_f k_f$, one can find the limit weight of the aggregated machine when its center of gravity is to the right of the point $a'_{md\,max}(a_v > a'_{vd\,max})$:

$$G'_{vd} = \frac{L(2q_r k_r - G_r) + G_c f_1 r_f - 2q_r k_r f_1\left(r_r - r_f\right)}{a_v + f_1 r_f} - \\ - R_y\left(1 + \frac{e}{a_v + f_1 r_f}\right) = G_{fd} - R_y\left(1 + \frac{e}{a_v + f r_f}\right) \quad (49)$$

In both cases:

$$a_v = \frac{\sum G_i a_i}{\sum G_i},\ G_v = \sum G_i,\ a_r = a_m + e \quad (50)$$

Since the effects of rolling resistance moments and the vertical component R_y on the loading of the front axle are mutually opposite, when determining the limit values of the aggregated machine's weight and the coordinate of its center of gravity, it is necessary to take into account the relationship between the normal reactions on the front axle of the unit in static and working positions.

The above relationships are valid for the case $Y'_{fd} > Y_f$. If $Y'_{fd} < Y_f$, then the boundary parameters are determined from the following system of equations:

$$G_m = \frac{L}{L - a_v}\left(2q_f k_f - G_f\right), \quad (51)$$

$$G'_{md} = \frac{L(2q_r k_r - G_r) + G_c f_1 r_f - 2q_r k_r f_1\left(r_r - r_f\right)}{a_m + f_1 r_f} - \\ - R_y\left(1 + \frac{e}{a_m + f_1 r_m}\right), \quad (52)$$

under the condition that $G'_{md} = G_m$. From the same considerations, the zone of possible placement of a

machine with a given weight G_m' on the chassis (TSSH) is determined.

If $Y_f > Y_{fd}'$, then when determining the possible range of the center of gravity position of the mounted machine, it is sufficient to consider only the static action of forces on the front axle:

$$a_{m1} = L\left(1 - \frac{2q_f k_f - G_f}{G_m'}\right) \le a_m \le a_{m2} = \frac{L(2q_r k_r - G_r) + G_c f_1 r_f - 2q_f k_f f_1 (r_r - r_f) - R_y(e + f_1 r_f) - G_m' f_1 r_f}{G_m' + R_y} \quad (53)$$

However, if $Y_f \le Y_{fd}'$, then when determining the zone of possible locations of the center of gravity of the mounted machine, it is necessary to take into account the dynamic redistribution of loads on the front axle:

$$a_{m1} = \frac{L(G_m' - 2q_f k_f + G_f) + (G_c + G_m') f_1 r_r + 2q_f k_f f_1 (r_r - r_f) + R_y(L - e - f_1 r_r)}{G_m' + R_y} \le a_m \le a_{m2} = \frac{L(2q_r k_r - G_r) - (G_c + G_m') f_1 r_f - 2q_r k_r f_1 (r_r - r_f) - R_y(e + f_1 r_f)}{G_m' + R_y} \quad (54)$$

A comparison of the calculated formulas for determining the maximum permissible weight of the attached machine and the coordinate of its center of gravity in the present case with the corresponding formulas for machines of the first group in the working position shows that they differ from the latter only by an additional term that accounts for the vertical component of the reactive soil resistance R_y.

Therefore, when determining the zone of possible positions of the center of gravity of the mounted machine, it is possible to use the load-carrying characteristic of the chassis (TSSH) obtained for machines of the first group in the working position (see Fig. 2), correspondingly reducing the ordinate G_m at each point approximately by the value of R_y. With increasing e, it is necessary to take into account the full value of the additional term in the calculation formulas.

Since the vertical component of the soil reaction on the working elements is a specific value for each machine, the load-carrying characteristic of the chassis (TSSH) obtained by superimposing R_y represents a particular case, whereas the corrected characteristic is universal.

For units with height-based control of tillage depth, the total vertical reaction on the chassis wheels is determined by:

$$Y_{fd}'' + Y_{rd}'' = G_c + (G_m + R_y) - Y_m \quad (55)$$

That is, due to the force effect of the mounted machine, it exceeds the weight of the chassis by an amount:

$$(G_m + R_y) - Y_m \quad (56)$$

When analysing the equilibrium conditions of the hinged section of the mounted machine (i.e. the working-tool sections with support wheels), it was shown that the vertical additional load on the chassis is created by the weight of the main frame of the mounted machine, which is rigidly fixed to the chassis frame, whereas the vertical component of the reactive soil resistance and the weight of the hinged section of the machine are borne primarily by the support wheels of the machine.

If the vertical component of the reactive soil resistance is directed upward, then to ensure stable machine operation, a combined (height-and-force) control method is used, in which the spring-type force regulator also participates in the vertical unloading of the chassis.

Thus, the transport condition of an aggregate with height-based tillage-depth control is the determining factor in calculating the load-carrying capacity of the chassis.

The redistribution of load to the rear driving wheels of the chassis within the load-carrying capacity of the tires under normal operating conditions ensures an increase in the traction efficiency coefficient. When considering the movement of the mounted machine within the calculated zone (the mounting distance between the front and rear wheels of the chassis) as a means of redistributing loads to the rear driving wheels, it is found that, from the standpoint of improving traction performance, the most favourable position of the mounted machine is at the boundary of this zone on the side of the driving wheels.

The position of the mounted machine on the chassis that satisfies both the principles of rational load-carrying capacity and the best traction–adhesion characteristics is determined by solving an optimization problem for the aggregate. An analysis of the overlapping of these zones showed that the optimal mounting zone corresponds to their complete coincidence. In this case, it is necessary to refine the longitudinal stability of the unit and the limiting calculated coordinates, which are constrained by the wheelbase dimensions of the chassis.

The efficiency of using a mounted machine increases with its weight and with the magnitude of displacement of the mounting zone, within limits allowed by the design and agrotechnical features of the aggregate.

By changing the track width of the chassis, it is possible to influence the position of the machine in cases where its displacement is limited by the stability of the unit. Combined with changes in the height of the mounted machine's center of gravity, determining its optimal position becomes a variational calculation problem.

The TSSH can be used with over 200 mounted and trailed machines and implements. For most of these, standard tires and rims meet the calculated load-carrying capacity of the chassis. However, when operating with mounted bulldozer blades, graders, front loaders, grapples, suspended rollers, and other heavy aggregates, the load on the front-wheel tires increases significantly. This causes a redistribution of loads onto the front axle and an increase in the corresponding reactions. Therefore, when aggregating with such machines, it is recommended to install wider rims and tires on the front wheels.

When performing field operations on over-moistened soils and meadows, for example, in land reclamation or mowing. It is advisable to install dual rear wheels to eliminate slippage and reduce soil compaction.

When a mobile crane unit (hook-lift system) is installed on the chassis instead of the cargo platform (or in place of a shortened version), outriggers are installed on the sides of the front axle to ensure aggregate stability and increase load-carrying capacity.

4. Conclusions

When machines and implements are mounted in the area between the front axle and the point of their center of gravity, their weight is limited by the load-carrying capacity of the front wheels, while the rear wheels remain underloaded. When the mounted machine is positioned between its center of gravity and the rear axle, the rear wheels become fully loaded, whereas the front wheels are underloaded. The action of rolling resistance moments results in a further reduction of the load on the front wheels.

During agricultural and forestry operations performed by the TSPCH on compacted soil after plowing, dynamic redistribution of loads significantly decreases the effective load-carrying capacity of the drive axle. In transport units based on the TSPCH used in municipal and road maintenance applications, the load-carrying capacity is close to the static value because the wheels move over firm or compacted surfaces. The load-carrying capacity of the TSPCH mounted platform corresponds to the calculated design value.

The developed method for calculating load-carrying capacity makes it possible to increase the chassis load-carrying capacity by up to 20%, or approximately 900 kg in numerical terms.

References

[1] Podrigalo M., Krasnokutskyi V., Selevych S., Vakhniuk S., Dolinskyi M. (2025) Methodology for Analyzing the Traction Dynamics of a Self-Propelled Tractor Chassis During Coupling with Cross-Axle Linkage of Mounted Machines, Innovations in Mechanical Engineering IV, 129-139, https://doi.org/10.1007/978-3-031-93554-1_12

[2] Lebedev, A., Shuliak, M., Lebedev, S., Khalin, S., Haidai, T., Kholodov, A., Pirogov, V., & Shaposhnyk, V. (2024). Determining conditions for providing maximum traction efficiency of tractor as part of a soil tillage unit. Eastern-European Journal of Enterprise Technologies, Volume 1(1 (127), pp. 6-14, 2024. doi: https://doi.org/10.15587/1729-4061.2024.297902.

[3] Podrigalo, M., Dubinin, Y., Moldovan, A., Polianskyi, O. et al., "New Methods and Systems for Monitoring the Functional Stability Parameters of Wheel Machines Power Units," SAE Technical Paper 2020-01-2014, 2020, https://doi.org/10.4271/2020-01-2014.

[4] Kozhushko, A., Tkachov, V., Mittsel, M., Sokolik, S. & Stanciu, D. (2024). Optimization of traction properties the electric tractor based on the simulation DLG-Powermix test cycles. International Journal of Mechatronics and Applied Mechanics, 15, pp. 70–78, 2024. doi: https://doi.org/10.17683/ijomam/issue14.5.

[5] İnce E., Güler M.A. (2020) On the advantages of the new power-split infinitely variable transmission over conventional mechanical transmissions based on fuel consumption analysis, Journal of Cleaner Production, 244, 118795, https://doi.org/10.1016/j.jclepro.2019.118795.

[6] Battiato A., Diserens E. (2017) Tractor traction performance simulation on differently textured soils and validation: A basic study to make traction and energy requirements accessible to the practice, Soil and Tillage Research, 166, 18-32, https://doi.org/10.1016/j.still.2016.09.005.

[7] Rebrov O., Kozhushko A., Kalchenko B., Mamontov A., Zakovorotniy A., Kalinin E., Holovina E. (2020) Mathematical model of diesel engine characteristics for determining the performance of traction dynamics of wheel-type tractor, EUREKA: Physics and Engineering, 4, 90 – 100. DOI: 10.21303/2461-4262.2020.001352

[8] Kutzbach H.D., Bürger A., Böttinger S. (2019) Rolling radii and moment arm of the wheel load for pneumatic tyres, Journal of Terramechanics, 82, 13-21, https://doi.org/10.1016/j.jterra.2018.11.002.

[9] Kumar S., Noori M.T., Pandey K.P. (2019) Performance characteristics of mode of ballast on energy efficiency indices of agricultural tyre in different terrain condition in controlled soil bin environment, Energy, 182, 48-56, https://doi.org/10.1016/j.energy.2019.06.043.

[10] Battiato A., Diserens E. (2017) Tractor traction performance simulation on differently textured soils and validation: A basic study to make traction and energy requirements accessible to the practice, Soil and Tillage Research, 166, 18-32, https://doi.org/10.1016/j.still.2016.09.005.

[11] Kozhushko, A., Tkachov, V., Horbov, O, Cioboată, D. (2024). Simulation of traction work to rationalise the weight distribution of the 4wd electric tractor. International Journal of Mechatronics and Applied Mechanics, 18, pp. 240–249, 2024. doi: https://doi.org/10.17683/ijomam/issue18.29

[12] Md-Tahir, H., Zhang, J., Xia, J., Chunling, Z., Hua, Z., & Yinghao, Z. (2019). Rigid lugged wheel for conventional agricultural wheeled tractors – Optimising traction performance and wheel–soil interaction in field operations. Biosystems Engineering, 188, 14-23. 10.1016/j.biosystemseng.2019.10.001

[13] Shafaei, S.M., Loghavi, M., & Kamgar, S. (2021). Fundamental realization of longitudinal slip efficiency of tractor wheels in a tillage practice. Soil & Tillage Research, 205, 104765. doi.org/10.1016/j.still.2020.104765.

[14] Shafaei, S.M., Loghavi, M., & Kamgar, S. (2021). Profound insight into tractor energy dissipation through inevitable interaction inside wheel-soil interface for the period of plowing works. Soil and Tillage Research. Volume 211, 104998, https://doi.org/10.1016/j.still.2021.104998.

[15] Janulevičius A., Damanauskas V. (2022) Prediction of tractor drive tire slippage under different inflation pressures, Journal of Terramechanics, 101, 23-31, https://doi.org/10.1016/j.jterra.2022.03.001.

[16] Lebedev, A.; Shuliak, M.; Khalin, S.; Lebedev, S.; Szwedziak, K.; Lejman, K.; Niedbała, G.; Łusiak, T. Methodology for Assessing Tractor Traction Properties with Instability of Coupling Weight. Agriculture 2023, 13, 977. https://doi.org/10.3390/agriculture13050977

[17] Artiomov N., Anikeev A., Kaluzhnij A., Sirovitskiy K., Kolodiazhnyi I. (2022) Investigation of agricultural unit loads in non-established mode of motion when performing technological operations, Engineering for Rural Development, 675 – 681. 10.22616/ERDev.2022.21.TF216